Green Chemistry

PAPER

View Article Online
View Journal | View Issue

Cite this: *Green Chem.*, 2025, **27**, 15135

Electrosynthesis of H_2O_2 aqueous solution beyond 30 wt% using sunlight, water and air

Yuefeng Qiu, Peng Jiang, Wenkai Ye, Jiahao Hu, Wenjie She, Bin Zhang, Tuo Ji, Liwen Mu, Xin Feng, Xiaohua Lu and Jiahua Zhu *

Received 25th July 2025,
Accepted 22nd October 2025

DOI: 10.1039/d5gc03867g

rsc.li/greenchem

The industrial anthraquinone process produces H_2O_2 solution with concentrations greater than 27.5 wt%; however, concerns regarding process safety, pollutant discharge and product purification remain. Here, we report an electrosynthesis system that directly produces H_2O_2 solution exceeding 30 wt% under ambient conditions using only sunlight, water and air. Benefiting from a carbon-based catalyst that achieves 17.86 mol g^{-1} h^{-1} H_2O_2 yield and up to 99.4% two-electron oxygen reduction reaction selectivity, the integrated electrosynthesis system can produce 30 wt% H_2O_2 continuously for more than 500 hours without noticeable degradation. Moreover, electronic-grade products were obtained without downstream purification. This work establishes an electrochemical route to produce high concentration and high-purity H_2O_2 that directly meets the needs of the chemical and semiconductor industries, advancing the electrification of chemical engineering processes in a sustainable way.

Green foundation

1. The industrial anthraquinone process produces H_2O_2 solution with concentrations greater than 27.5 wt%, yet no existing photo/electrochemical technologies can produce H_2O_2 solution beyond 20 wt%. This work directly synthesizes H_2O_2 solution at concentrations beyond the industrial level (>27.5 wt%) with only electricity, air and water.
2. In this work, we developed a highly efficient carbon-based catalyst that enables exceptional yield and selectivity in electrosynthesis of H_2O_2. The catalyst was then integrated into a membrane electrode and packed in a stack reactor; 30 wt% H_2O_2 aqueous solution can be continuously produced for more than 500 hours without noticeable degradation. By integrating a solar panel with the electrochemical H_2O_2 unit, a self-powered H_2O_2 production system was established and field tests were carried out to demonstrate the feasibility of the design.
3. This work can be enhanced as a more environmentally friendly process in several ways. The design of novel catalysts could eliminate the need for precious metals, membrane electrodes could be substituted with more sustainable materials, and reactor configurations could be optimized to boost reaction yield and efficiency.

Introduction

Hydrogen peroxide (H_2O_2) is a crucial chemical widely utilized in sterilization, paper bleaching, environmental remediation, and chemical production.[1,2] Currently, industrial manufacturing of H_2O_2 primarily relies on the anthraquinone (AQ) process,[3] which poses significant risks of explosion in the hydrogenation, oxidation and distillation steps and also environmental harm due to the generation and discharge of carcinogenic anthraquinone.[4,5]

The direct electrosynthesis of H_2O_2 through a two-electron oxygen reduction reaction ($2e^-$ ORR) has emerged as a safer, simpler and more environmentally friendly alternative.[6,7] Flow cells with gas diffusion layers were earlier used to produce H_2O_2, but due to the solubility of oxygen in electrolyte solution, the concentration and purity of the product were unsatisfactory.[8] In 2019, Wang *et al.*[9] reported an electrosynthesis method that produced 20 wt% H_2O_2 aqueous solution using solid electrolyte in flow cells. This process involves two half-reactions (cathode: $O_2 + H_2O + 2e^- \rightarrow HO_2^- + OH^-$; anode: $H_2 - 2e^- \rightarrow 2H^+$) and effectively prevents contact between hydrogen and oxygen, thus enhancing safety and eliminating organic impurities and potential pollutions.[10] However, there is a pressing need to further increase H_2O_2 concentrations to industrial levels, such as 27.5 wt% and beyond. Achieving this remains a significant challenge, with the development of efficient catalysts being one of the key hurdles to overcome. Modification of carbon[11,12] seems a promising approach to achieve satisfactory $2e^-$ ORR selectivity,[13] while it often

State Key Laboratory of Materials-Oriented Chemical Engineering, College of Chemical Engineering, Nanjing Tech University, Nanjing, 211816, P. R. China. E-mail: jhzhu@njtech.edu.cn

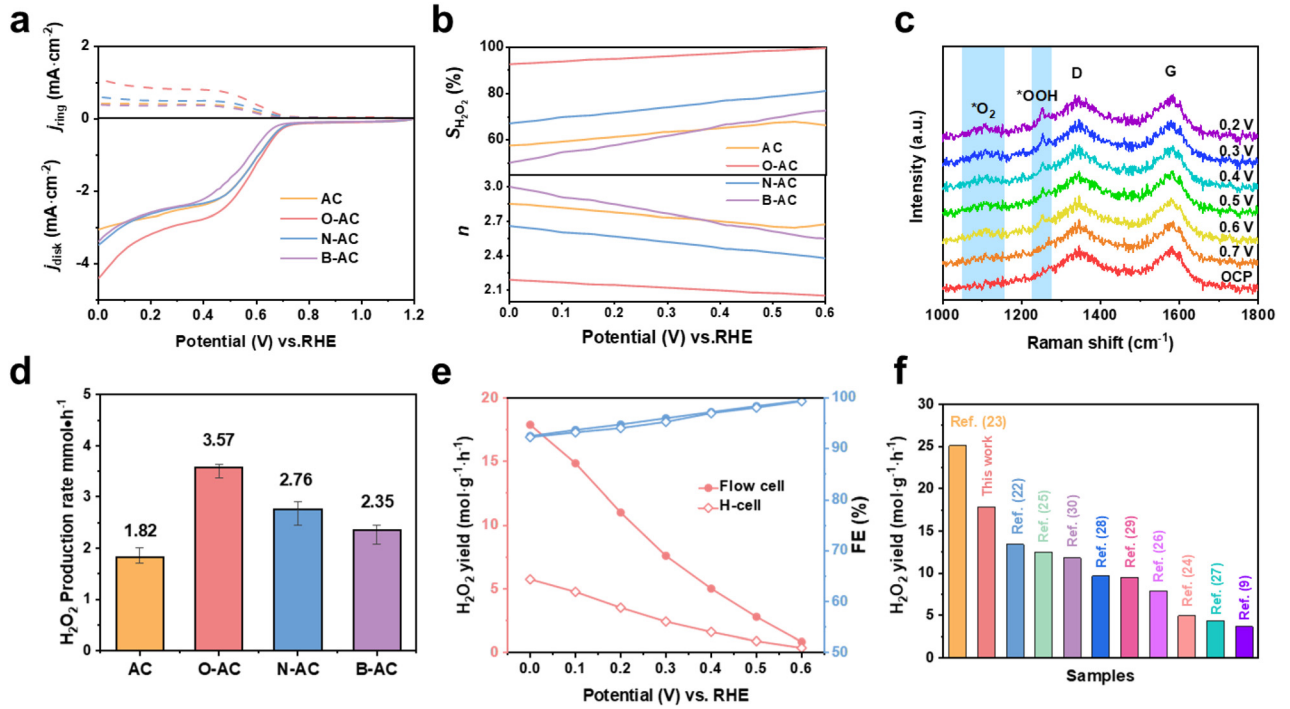

Fig. 1 (a) ORR polarization curves on a RRDE; solid and dashed lines represent the disk and ring current densities (j_{disk} and j_{ring}), respectively; (b) H_2O_2 selectivity and the corresponding electron transfer number; (c) *in situ* Raman spectroelectrochemistry during the ORR measurements of O-AC; (d) H_2O_2 production rate of all catalyst samples; (e) H_2O_2 yield and Faraday efficiency (FE) of O-AC in the H-cell and flow cell; and (f) comparison of the H_2O_2 yield with recently reported catalysts (comparative data references: 9 and 22–30).

damages the graphite domain and thus corrupted the electron conduction pathway. Therefore, there is still ongoing research to develop 2e$^-$ ORR catalysts that offer higher yield and selectivity to produce H_2O_2 in a more efficient way.[14–16]

In addition, as we transition from fossil fuels to sustainable electricity sources like solar and wind power, there is a strong push to integrate electricity and transform traditional chemical engineering processes into greener and safer alternatives.[17] However, the intermittent nature of sustainable energy poses challenges for its integration into existing processes, as consistent and continuous operation is crucial for chemical engineering.[18] While converting green electricity to hydrogen has gained traction, issues related to the storage and transportation of hydrogen remain.[19] A more practical approach is to utilize sustainable electricity for the production of chemicals and liquid fuels;[20] however, options are constrained by technological readiness, economic viability, and environmental factors.

Here, we report an integrated solar-powered electrosynthesis system directly transforming H_2O to 30 wt% H_2O_2 aqueous solution without an external energy supply. Specifically, a high-selectivity, high-yield 2e$^-$ ORR catalyst was synthesized using low-temperature plasma. When integrated into a continuous flow electrochemical reactor, an H_2O_2 aqueous solution with concentrations exceeding 30 wt% can be achieved, satisfying the industrial standards without additional concentration. With environmental and pipeline upgrading, electronic grade products can be produced without any purification processes. In addition, a solar powered system was developed for continuous production of green H_2O_2 without relying on external power. Moreover, techno-economic analysis (TEA) and life-cycle assessment (LCA) were conducted based on the established system.

Results and discussion

To realize high-concentration H_2O_2 production, the 2e$^-$ ORR selectivity and H_2O_2 yield of the cathode catalyst are essential. Conventional wet-chemical modification of the carbon catalyst can enhance selectivity,[9] while it sacrifices the intrinsic conductivity of the carbon framework. Here, we used a low-temperature plasma technology to tune surface functionality while retaining the bulk electrical conductivity of carbon. A series of elements, such as oxygen (O), nitrogen (N) and boron (B), were doped onto the carbon surface (for elemental analysis, refer to Fig. S1) and their ORR performance was assessed using a rotating ring-disk electrode (RRDE) at 1600 rpm in an O_2-saturated 0.1 M Na_2SO_4 electrolyte. The corresponding ORR polarization curves for these catalysts are shown in Fig. 1a. The O-AC catalyst demonstrated a higher ring current density (1.08 mA cm^{-2}) and a more positive onset potential (0.70 V) compared to the other samples (0.38–0.60 mA cm^{-2} and 0.64–0.68 V), indicating significant H_2O_2 production activity. According to the Koutecky–Levich equation, O-AC exhibited a value of n close to 2 and a

H_2O_2 selectivity of 99.4% at 0.6 V (Fig. 1b). Furthermore, O-AC demonstrated remarkable selectivity over a broad voltage range of 0–0.6 V, significantly surpassing the other catalysts (57.6–81.2%). It showed marginally improved reaction kinetics and outstanding ORR activity (Fig. S2 and S3).

To understand the reaction process, *in situ* Raman spectra were recorded on the catalysts at various potentials using an electrolytic cell (refer to Fig. 1c for O-AC and refer to Fig. S4 for the others). Besides the characteristic D band (1350 cm^{-1}) and G band (1580 cm^{-1}) of the carbon substrate,[12] a broad peak around 1100 cm^{-1} was observed, attributed to the adsorption of oxygen molecules on the catalyst surface and initial electron transfer.[21] A peak at 1250 cm^{-1}, associated with the vibration of *OOH, was observed for O-AC at 0.6 V,[22] aligning with the previously noted most positive onset potential for O-AC. In terms of the H_2O_2 production rate, O-AC exhibited the highest rate of 3.57 mmol h^{-1} among the tested catalysts (Fig. 1d). As current density increased, the H_2O_2 production rate approached linear growth, with only a slight decrease in Faraday efficiency (FE) observed at a current density of 100 mA cm^{-2} (Fig. S5). Following optimization, O-AC achieved H_2O_2 yields of 17.86 mol g^{-1} h^{-1} in a flow cell and 5.75 mol g^{-1} h^{-1} in an H-cell, both with Faraday efficiencies exceeding 92% (Fig. 1e). O-AC in this work demonstrated outstanding performance, compared with previously reported catalysts[9,22–30] (Fig. 1f).

To meet industrial production requirements, the reactor size was scaled up from 4 cm^2 to 625 cm^2 (Fig. 2a–c). For each reactor size, the H_2O_2 concentration and FE were monitored at various water flow rates (Fig. 2d–f). Decreasing the water flow rate led to an increase in H_2O_2 concentration, reaching values from 1.96 wt% to 36.76 wt% in the 625 cm^2 reactor (Fig. 2f). A noticeable drop in the FE occurred once the H_2O_2 concentration exceeded 5–10 wt% in all reactors of different sizes. Specifically, the FE for producing 30 wt% H_2O_2 dropped to 51.1%. This decline may be attributed to the disrupted balance between high-concentration H_2O_2 and the oxygen reduction reaction, causing a shift from the $2e^-$ process to the $4e^-$ process, thus resulting in lower selectivity. Additionally, H_2O_2 decomposition is likely to occur at high concentration, which is evidenced by the appearance of oxygen columns in the pipeline of the outlet stream.

Fig. 3a illustrates the main flow of materials through two reactors, where water is fed into the electrolysis system (using a commercial PEM reactor in this work) to produce hydrogen and oxygen. To maintain a 1 : 1 molar ratio of hydrogen to oxygen, a separate stream of oxygen or air was supplied to the H_2O_2 electrochemical (EC) reactor. The detailed structure of the EC reactor is shown in Fig. 3b, where O-AC and platinum carbon (Pt/C) served as the cathode and anode catalysts, respectively. The catalysts, along with the exchange membranes (PEM and AEM) and gas diffusion layers (GDLs), were assembled into two membrane electrodes, positioned on both sides of a partition filled with a solid electrolyte. Hydrogen and oxygen were introduced to both sides of the reactor, while ultrapure water was discharged through the solid electrolyte,

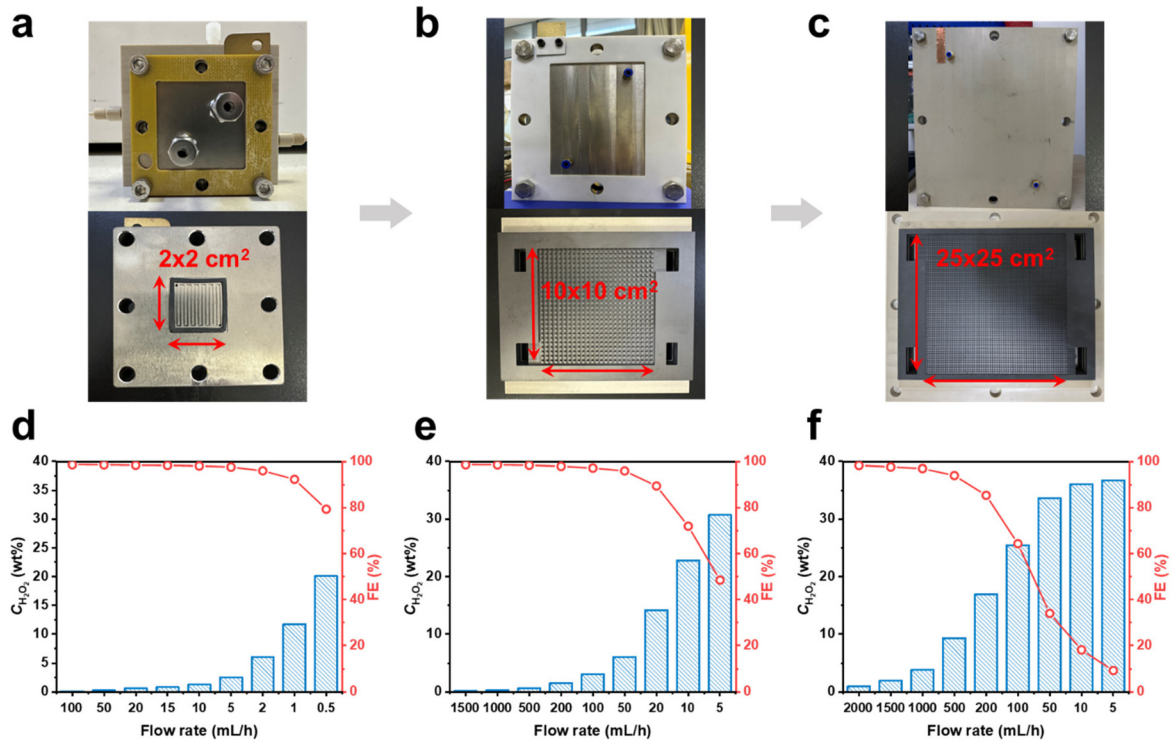

Fig. 2 (a–c) Scaling up of the H_2O_2 reactor with different dimensions of 4, 100 and 625 cm^2 and (d–f) the variation of H_2O_2 concentration and FE as a function of flow rate on different-sized reactors.

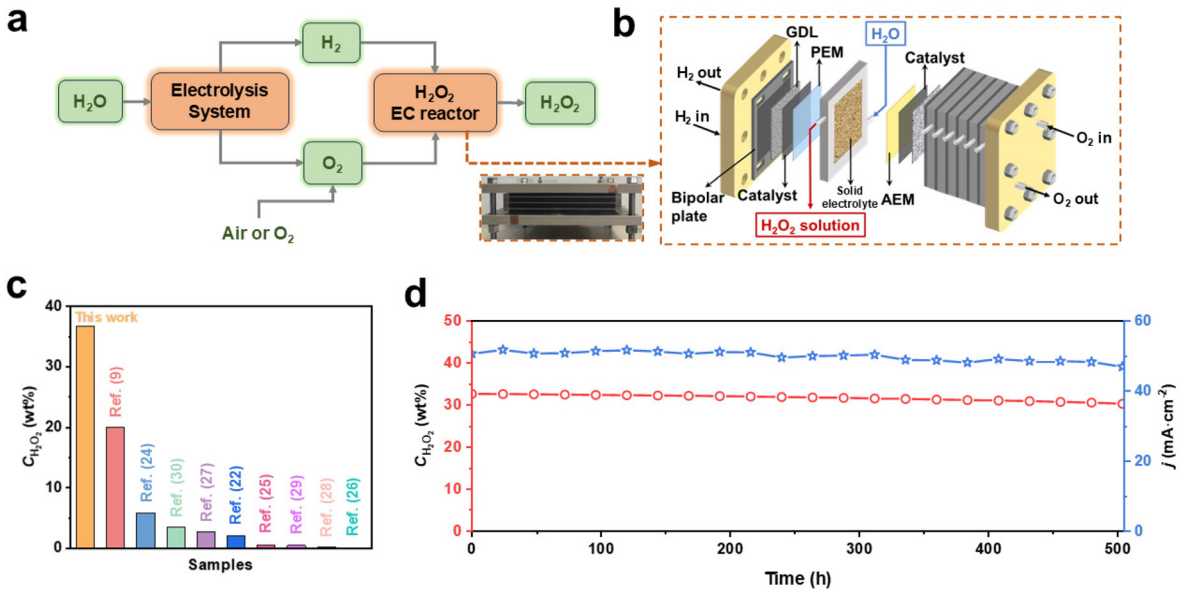

Fig. 3 (a) The schematic illustration of the reaction process, (b) diagram of the H_2O_2 electrochemical reactor stack, (c) comparison of H_2O_2 concentration obtained in this work with those in other literature reports (refs. 9, 22 and 24–30), and (d) stability evaluation for 500 hours by monitoring H_2O_2 concentration and FE (reactor size: 100 cm^2).

carrying away the produced H_2O_2 to form an aqueous solution (Fig. 3b). A maximal H_2O_2 concentration of 36.76 wt% can be produced, which is the highest reported value so far[9,22–30] (Fig. 3c).

To assess the stability of the reactor system, experiments were conducted with H_2O_2 output concentrations of approximately 30 wt% over a continuous period of 500 hours (Fig. 3d). The results showed that the H_2O_2 concentration remained consistently above 30 wt%, with only a slight decrease in current density after 500 hours of operation. Furthermore, by placing the reaction system in a clean room and upgrading the pipeline, ultrapure H_2O_2 aqueous solutions were produced. The quality indicators of the produced H_2O_2 solution, including the concentration, free acid, total organic carbon, and metal ions, are summarized in Table 1 (with further details in Tables S2–11), demonstrating the capability of the reactor system in producing electronic grade H_2O_2 solution without any purification steps. Indicators for different grades of H_2O_2 solution were also provided for comparison. It is important to note that the concentration of free acid and total organic carbon in this work is two orders of magnitude lower than the electronic grade (G5) standard, highlighting its distinct advantage over existing technologies.

To address the intermittent nature of sustainable electricity and the continuous energy demands of the reactor, a solar powered electrosynthesis system for continuous H_2O_2 production was designed. This system consists of a solar panel, an energy storage module, and an H_2O_2 production unit (Fig. 4a–c). The entire system was tested onsite at the Nanjing Tech University campus for over twelve days from March 15 to 26, 2025. Daily records were kept of weather conditions, solar power generation, battery power levels, and H_2O_2 concentration (Fig. 4d). During daylight hours, the solar panel generated electricity, which was stored in the battery. At night, the battery supplied energy to the H_2O_2 production unit, ensuring continuous synthesis. The battery charge level fluctuated between 10% and 100%, demonstrating its ability to buffer energy generation and consumption for the H_2O_2 production unit. Throughout the twelve days of operation, the production line consistently delivered H_2O_2 solutions with concentrations above 30 wt%, demonstrating its capability to deliver reliable performance (Fig. 4d).

To perform TEA and LCA, the electrochemical production (EP) process of electronic grade H_2O_2 was developed using Aspen Plus V14 based on experimental data. For comparison, a conventional production (CP) process was also established,

Table 1 Main quality indicators of H_2O_2 solution of different grades

	Industrial grade	Medical grade	Food grade	Electronic grade (G5)	This work
H_2O_2 concentration (wt%)	≥27.5	1–6	≥35	≥30	≥30
Free acid (ppb)	≤400 000	≤400 000	≤50 000	≤30	<0.1
Total organic carbon (ppm)	≤250 000	≤250 000	≤80	≤10	<0.1
Metal ions (ppb)	≤200 000	≤1000	≤500	≤0.01	<0.001

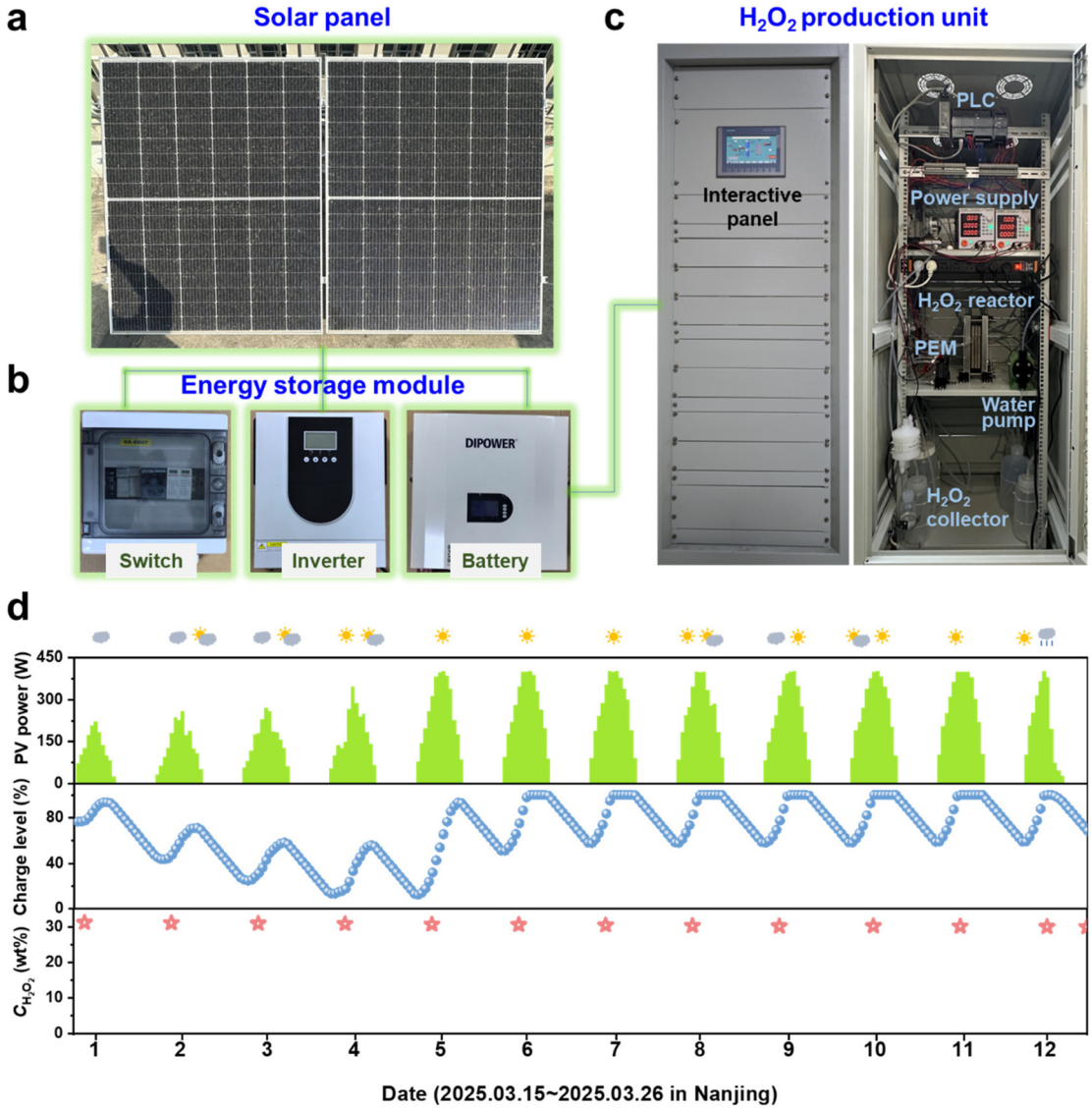

Fig. 4 The solar-power driven electrosynthesis system for continuous production of aqueous H_2O_2 solution. (a) Solar panel, (b) energy storage model consisting of a switch, an inverter and a battery, (c) H_2O_2 production unit, and (d) continuous on-site operation for twelve days under different weather conditions with recorded photovoltaic power generation, battery charge level and H_2O_2 concentration.

integrating the AQ process for H_2O_2 production with an ultra-purification step to achieve electronic-grade quality. Detailed process descriptions and calculation details are provided in Tables S12 and S23. Both processes were designed to achieve an annual H_2O_2 output of 100 000 tons, assuming 8000 hours of operation per year (for details, refer to Fig. S6–S11). Fig. 5a and b present the mass flow of the reaction species involved in the EP and CP processes, based on an H_2O_2 production rate of 12 500 kg h^{-1}. The EP process directly produced electronic-grade H_2O_2 without purification, reducing raw material consumption and eliminating wastewater treatment compared to the CP process. Furthermore, the EP process decreased energy consumption by 14.02%, mainly by eliminating the energy needed for concentration and purification, which were required in the CP process (Fig. 5c).

Fig. 5d compares the production costs of H_2O_2 for the EP and CP processes. The EP process achieved a lower cost of USD 189.92 per ton, which is a 32.88% reduction compared to the CP process. This cost advantage is primarily due to the elimination of the complex concentration and purification steps, allowing for the direct production of 30% electronic-grade H_2O_2. This study also demonstrated economic benefits over previous reports, such as Zhang *et al.*[30] (233.40 USD per t for 3 wt%) and Xia *et al.*[9] (340 USD per t for 20 wt%). The main contributors to costs were the capital investment of electrochemical equipment (40.03%) and electricity consumption (36.22%). Fig. 5e presents a sensitivity analysis, identifying faradaic efficiency, current density, and electrolyzer cost as the key cost drivers. With improvements in electrochemical equipment and the increasing availability of green electricity, the

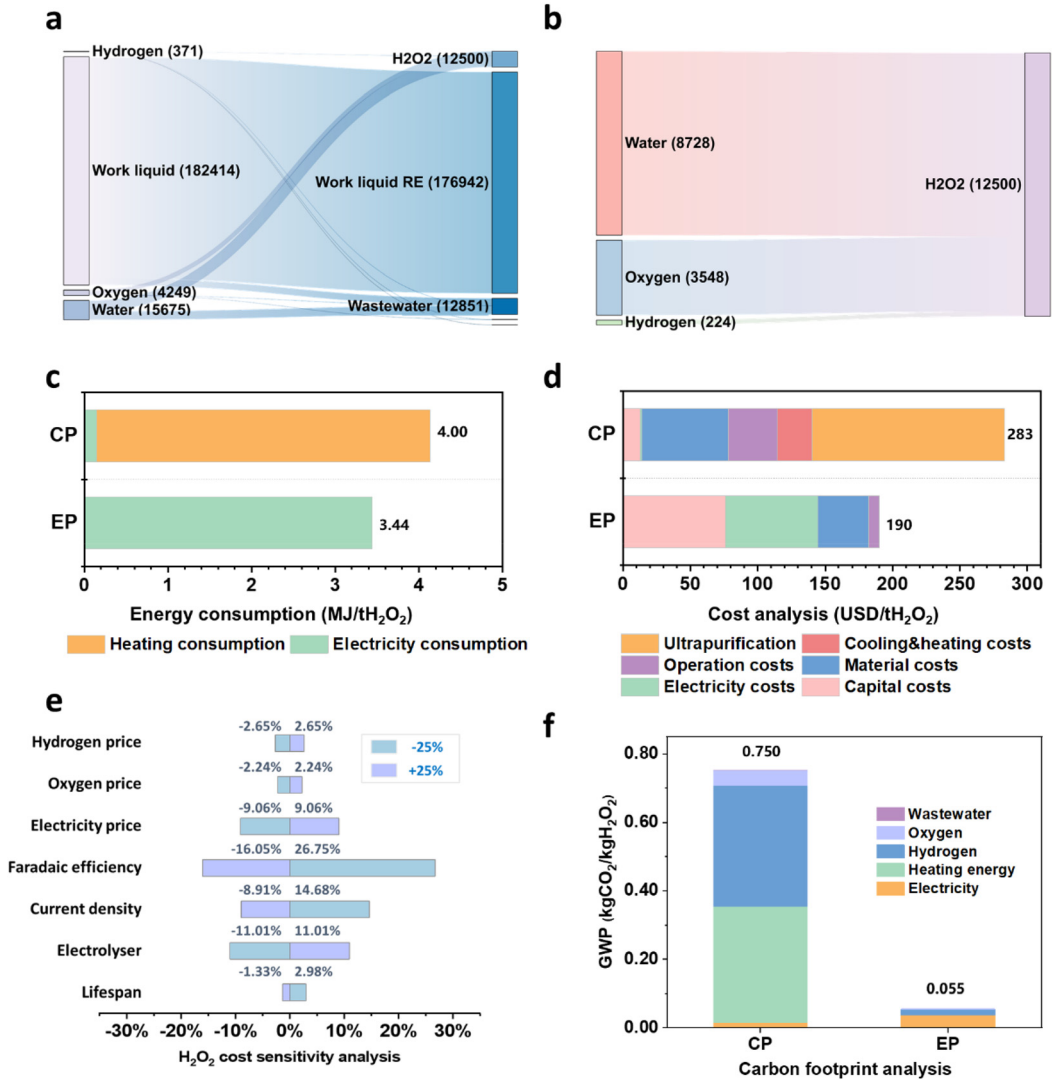

Fig. 5 Mass flow, energy consumption, H_2O_2 cost, and LCA analysis of electrochemical (EP) and conventional (CP) processes, including (a and b) mass flow Sankey diagrams with the production of 12 500 kg h^{-1} H_2O_2 as a benchmark, (c) energy consumption, (d) cost estimation, (e) H_2O_2 cost sensitivity analysis, and (f) carbon footprint comparison.

costs of H_2O_2 are expected to decrease further. Moreover, the EP process demonstrated environmental advantages (Fig. 5f), with a GWP of 0.055 kg CO_2e per kg H_2O_2, significantly lower than that of the CP process (0.750 kg CO_2e per kg H_2O_2).

Conclusions

By offering a complete green approach for producing H_2O_2 using sustainable resources (light, water, and air) and ensuring that the product meets industrial requirements, this work serves as a unique example of connecting intermittent electricity with liquid chemicals. The integrated electrosynthesis system can produce 30 wt% H_2O_2 continuously for more than 500 hours with a 17.86 mol g^{-1} h^{-1} H_2O_2 yield and 99.4% $2e^-$ ORR selectivity catalyst. Furthermore, the adaptable design of the reaction module allows for the implementation of a customized H_2O_2 production unit for localized production. The TEA and LCA results indicated that this new process is more economical with lower carbon emissions compared to the anthraquinone process.

Author contributions

Y. Qiu: data curation, methodology, and writing – original draft; P. Jiang: investigation, methodology, and writing – original draft; W. Ye: formal analysis and validation; J. Hu: investigation and methodology; W. She: data curation and validation; B. Zhang: formal analysis, investigation and validation; T. Ji: data curation, validation and funding acquisition; L. Mu: investigation and formal analysis; X. Feng: project administration; X. Lu: investigation and project administration; and J. Zhu: conceptualization, funding acquisition, supervision, and writing – review & editing.

Conflicts of interest

There are no conflicts to declare.

Data availability

The data supporting this article have been included as part of the supplementary information (SI). Supplementary information is available. See DOI: https://doi.org/10.1039/d5gc03867g.

Acknowledgements

The authors appreciate the financial support from the National Key Research and Development Program of China (2024YFE0206200) and the National Natural Science Foundation of China (22378183 and 22378184).

References

1 Y.-Y. Yan, W.-J. Niu, W.-W. Zhao, R.-J. Li, E.-P. Feng, B.-X. Yu, B.-K. Chu and C.-Y. Cai, *Adv. Energy Mater.*, 2024, **14**, 2303506.
2 N. Wang, S. Ma, P. Zuo, J. Duan and B. Hou, *Adv. Sci.*, 2021, **8**, e2100076.
3 S. Yang, A. Verdaguer-Casadevall, L. Arnarson, L. Silvio, V. Colic, R. Frydendal, J. Rossmeisl, I. Chorkendorff and I. E. L. Stephens, *ACS Catal.*, 2018, **8**, 4064–4081.
4 J. S. J. Hargreaves, Y. M. Chung, W.-S. Ahn, T. Hisatomi, K. Domen, M. C. Kung and H. H. Kung, *Appl. Catal., A*, 2020, **594**, 117419.
5 F. Menegazzo, M. Signoretto, E. Ghedini and G. Strukul, *Catalysts*, 2019, **9**, 251.
6 X. Sun, J. Yang, X. Zeng, L. Guo, C. Bie, Z. Wang, K. Sun, A. K. Sahu, M. Tebyetekerwa, T. E. Rufford and X. Zhang, *Angew. Chem., Int. Ed.*, 2024, **63**, e202414417.
7 D. W. Flaherty, *ACS Catal.*, 2018, **8**, 1520–1527.
8 E. Jung, H. Shin, W. H. Antink, Y. Sung and T. Hyeon, *ACS Energy Lett.*, 2020, **5**, 1881–1892.
9 C. Xia, Y. Xia, P. Zhu, L. Fan and H. Wang, *Science*, 2019, **366**, 226–231.
10 S. C. Perry, D. Pangotra, L. Vieira, L.-I. Csepei, V. Sieber, L. Wang, C. P. de Leon and F. C. Walsh, *Nat. Rev. Chem.*, 2019, **3**, 442–458.
11 G. F. Han, F. Li, W. Zou, M. Karamad, J.-P. Jeon, S.-W. Kim, S.-J. Kim, Y. Bu, Z. Fu, Y. Lu, S. Siahrostami and J.-B. Baek, *Nat. Commun.*, 2020, **11**, 2209.
12 S. Chen, T. Luo, K. Chen, Y. Lin, J. Fu, K. Liu, C. Cai, Q. Wang, H. Li, X. Li, J. Hu, H. Li, M. Zhu and M. Liu, *Angew. Chem., Int. Ed.*, 2021, **60**, 16607–16614.
13 Y. Guo, R. Zhang, S. Zhang, H. Hong, Y. Zhao, Z. Huang, C. Han, H. Li and C. Zhi, *Energy Environ. Sci.*, 2022, **15**, 4167–4174.
14 C. Zhang, P. Shan, Y. Zou, T. Bao, X. Zhang, Z. Li, Y. Wang, G. Wei, C. Liu and C. Yu, *Nat. Sustain.*, 2025, **8**, 542–552.
15 Y. Gu, Y. Tan, H. Tan, Y. Han, D. Cheng, F. Lin, Z. Qian, L. Zeng, S. Zhang, R. Zeng, Y. Liu, H. Guo, M. Luo and S. Guo, *Nat. Synth.*, 2025, **4**, 614–621.
16 Q. Huang, B. Xia, M. Li, H. Guan, M. Antonietti and S. Chen, *Nat. Commun.*, 2024, **15**, 4157.
17 P. De Luna, C. Hahn, D. Higgins, S. A. Jaffer, T. F. Jaramillo and E. H. Sargent, *Science*, 2019, **364**, eaav3506.
18 J. Qi, Y. Du, Q. Yang, N. Jiang, J. Li, Y. Ma, Y. Ma, X. Zhao and J. Qiu, *Nat. Commun.*, 2023, **14**, 6263.
19 O. Smith, O. Cattell, E. Farcot, R. D. O'Dea and K. I. Hopcraft, *Sci. Adv.*, 2022, **8**, eabj6734.
20 K. M. Van Geem, V. V. Galvita and G. B. Marin, *Science*, 2019, **364**, 734–735.
21 G. Ye, S. Liu, K. Zhao and Z. He, *Angew. Chem., Int. Ed.*, 2023, **62**, e202303409.
22 Z. Song, X. Chi, S. Dong, B. Meng, X. Yu, X. Liu, Y. Zhou and J. Wang, *Angew. Chem., Int. Ed.*, 2024, **63**, e202317267.
23 Y. Wu, Y. Zhao, Q. Yuan, H. Sun, A. Wang, K. Sun, G. I. N. Waterhouse, Z. Wang, J. Wu, J. Jiang and M. Fan, *Nat. Commun.*, 2024, **15**, 10843.
24 C. Li, K. Yu, A. Bird, F. Guo, J. Ilavsky, Y. Liu, D. A. Cullen, A. Kusoglu, A. Z. Weber, P. J. Ferreira and J. Xie, *Energy Environ. Sci.*, 2023, **16**, 2977–2990.
25 H. Xu, S. Zhang, X. Zhang, M. Xu, M. Han, L. R. Zheng, Y. Zhang, G. Wang, H. Zhang and H. Zhao, *Angew. Chem., Int. Ed.*, 2023, **62**, e202314414.
26 R. D. Ross, K. Lee, G. J. Q. Cintron, K. Xu, H. Sheng, J. R. Schmidt and S. Jin, *J. Am. Chem. Soc.*, 2024, **146**, 15718–15729.
27 C. Zhang, L. Yuan, C. Liu, Z. Li, Y. Zou, X. Zhang, Y. Zhang, Z. Zhang, G. Wei and C. Yu, *J. Am. Chem. Soc.*, 2023, **145**, 7791–7799.
28 J. Du, G. Han, W. Zhang, L. Li, Y. Yan, Y. Shi, X. Zhang, L. Geng, Z. Wang, Y. Xiong, G. Yin and C. Du, *Nat. Commun.*, 2023, **14**, 4766.
29 Q. Zhi, R. Jiang, X. Yang, Y. Jin, D. Qi, K. Wang, Y. Liu and J. Jiang, *Nat. Commun.*, 2024, **15**, 678.
30 M.-D. Zhang, J.-R. Huang, C.-P. Liang, X.-M. Chen and P.-Q. Liao, *J. Am. Chem. Soc.*, 2024, **146**, 31034–31041.